Journal of Applied Mechanics and Technical Physics, Vol. 44, No. 6, pp. 760–769, 2003

CUMULATION OF SEISMIC WAVES DURING FORMATION OF KIMBERLITE PIPES

V. A. Simonenko and N. I. Shishkin

UDC 539.8; 551.1/.4; 525.23

A possible mechanism of formation of kimberlite pipes is considered. It is shown that they could have formed upon impact of a large cosmic body on the Earth in the impact's antipode region during focusing of seismic surface waves. It is established that convergence of a surface wave to the antipode region is accompanied by an increase in the wave amplitude and the wave energy density. Focusing of such a wave results in an almost vertical rupture of the Earth's crust and formation of a channel diverging to the surface — a burst pipe. Along this channel, kimberlite magma, additionally heated by deep focusing of the other waves, rises to the Earth's surface to form a kimberlite pipe. The absence of ideal cylindrical symmetry due to the inhomogeneity of the Earth's crust along the path of wave propagation leads to wave defocusing and formation of several centers of convergence, i.e., formation of a pipe field.

Key words: *kimberlite pipe, cumulation of seismic waves, antipodes, rock failure.*

Introduction. In the ideal case of a convergent cylindrical wave in an elastic medium, the wave amplitude and energy density increase without bound. In the domestic literature, such phenomena are called cumulative [1]. Energy cumulation during wave convergence to the focusing center or axis occurs in real media, too. This is also characteristic of convergent seismic Rayleigh and Lové waves, because in the neighborhood of their focusing axes, the motion becomes axisymmetric.

Favorable conditions for cumulation of seismic surface waves are produced by impacts of rather large cosmic bodies on the Earth. The surface waves generated by such impacts are focused in the region that is diametrically opposite to the impact region — the antipode region. An increase in the wave energy density during wave convergence leads to crustal rock failure near the wave focusing axis. One might expect geophysical consequences of these phenomena, in particular, formation of geological structures such as kimberlite pipes (KPs) or other burst pipes.

Kimberlite pipes are a variety of burst pipes or diatremes and are bell-mouthed vertical channels in the Earth's crust filled with endogenous rocks. They have round, elongated or irregular cross sections with a surface area of 10^2 to $1.4 \cdot 10^6$ m^2. With increase in the depth, the cross-sectional area decreases, and at depths of 1–3 km, the pipes usually pass into dikes — bedding, steeply dipping formations of large extent and small thickness [2]. Dikes are feeder channels for the pipes and join them to the deep-seated faults of the Earth.

As a rule, KPs are located on the shields of ancient plates (cratons) — the hardest segments of the Earth's crust, closer to the crustal blocks, whose rocks exhibit fine, isometrically oriented, tectonic fracture. Within a kimberlite province, the pipes are grouped into kimberlite fields, whose typical dimensions range from a few to several tens of kilometers. Within the same field there may be three to several tens of pipes. For example, in the Central Siberian kimberlite province, the Malobotuobin field contains nine pipes and the Daldyn field contains 55 pipes [2]. The distance between the pipes ranges from a few hundred meters to several kilometers.

Kimberlite is an ultrabasic porphyritic rock which includes pyrope-containing rocks: peridotites, pyroxenes, etc. Peridotites are the main components of the Earth's mantle [3]. Besides being of economical value (diamond fields), kimberlite rocks filling pipes and feeder dikes are of considerable scientific interest. They contain information on the origin of diamonds, rock composition, and thermodynamic conditions in the upper mantle of the Earth.

Institute of Engineering Physics, Snezhinsk 456770. Translated from Prikladnaya Mekhanika i Tekhnicheskaya Fizika, Vol. 44, No. 6, pp. 12–24, November–December, 2003. Original article submitted November 19, 2002; revision submitted April 16, 2003.

 0021-8944/03/4406-0760 $25.00

Kimberlite pipes have the following features [2, 4]. The top of the pipes (bell mouth) has the shape of a truncated cone with its broad base facing the day surface that existed at the moment of formation of the pipe. The middle part of a pipe has a nearly circular cross section, which slowly converges as the depth increases. The bottom (root) segment has less regular structure. Its cross section decreases with increase in the depth, the pipe is flattened, and at a depth of 1–3 km, it passes into feeder dikes. Originally, the horizontal rock beds near the pipes are curved upward or downward or remain horizontal. In the contact zone adjacent to the pipe, the rocks are partitioned by systems of vertical, concentric, and radial cracks propagating at a distance of several (sometimes, tens) meters from the contact. Kimberlite intruded into the cracks forms apophysises —- thin vein-like branches.

Kimberlite in pipes are predominantly breccias, i.e., they consist of consolidated fragments of different rocks, whereas in feeder dikes and sills (bedding interstitial formations), they are massive. At the tops of the pipes, kimberlites contain large aggregates of fragments and blocks of enclosing rocks, which could have formed upon fall of the channel sides and have moved downward several hundred meters (sometimes, up to 1 km). Plutonic xenoliths present in kimberlites (peridot, garnet, diopside, diamond, quartz, etc.) exhibit metamorphism — partial or complete recrystallization, change in mineral composition, etc. They can include high-pressure quartz phases (koesite and stishovite), lonsdalite (a variety of diamond), and a variety of other minerals. One more important feature of kimberlites found in the geological complexes in question is that traces of thermal action are absent on the enclosing rocks and xenoliths in the pipes but are present on the contact boundaries of dikes and sills. This implies that kimberlites intruded into the pipes in a cold state [4].

The physical properties and mineralogical composition of kimberlites and xenoliths contained in them indicate that they originated at a great depth and ascended at a velocity. Laboratory studies of mantle rocks at high pressures show that kimberlite magmas should originate in the lower layers of the hard lithosphere at depths of 120–190 km [5].

According to the estimate in [6], the ascent velocity of xenoliths in the pipe channels could have reached 100 km/h. The intrusion of kimberlites into the pipes of Southern Africa, beginning with the Precambrian, occurred about 1700, 1200, 100, and 80 million years ago. In the pipes of the Siberian platform, kimberlite intrusion occurred 470, 375, 325, and 200 million years ago, and in the pipes of the Russian platform, 355 million years ago [7]. It is generally agreed that kimberlite pipes are the terminal segments of transport channels along which the mantle material rose to the Earth's surface.

The formation mechanism of KPs is still unclear and is a subject of controversy. There are a number of hypotheses on their origin [2]. We consider the main of them.

The earliest hypothesis proposed by Wagner [8] states that KPs result from a number of gas bursts. Mikheenko [9] suggests that KPs result from diapiric piercing of rocks and kimberlite bodies are diapirs or stocks. Novikov and Slobodskoi [10] argue that diatremes are formed by gas abrasion of enclosing rocks. Milashev [2] and Wagner [8] state that KPs are vents of ancient volcanos. Dawson [4] discusses the mechanism of KP formation during fluidization, where detrital material is transported by a fast moving gas–liquid stream (the gas is a mixture of carbon dioxide and water vapor and the liquid is kimberlite magma enriched with calcite). Vladimirov et al. [11] consider the mechanism of KP formation via fluid brecciation. Under fluid brecciation Vladimirov et al. [11] understand a number of processes playing, in their opinion, an important role in the formation of pipes: hydraulic splitting and pushing apart of enclosing rocks by interstitial liquid or gas–liquid kimberlites; decrease in hardness due to adsorption and stress corrosion of enclosing rocks, caused by fluid kimberlite and leading to rock failure; gas and gas–liquid abrasion of enclosing rocks. (Stress corrosion implies corrosion at the interfaces between media due to the presence of stresses.) In addition, it is assumed [11] that one of the determining factors of KP formation is the failure of enclosing rocks that existed before filling.

According to [12, 13], diatremes result from the action of uprising solutions, which partly dissolve enclosing rocks along subvertical channels, leading to failure of rock blocks and formation of pipes. It is stated [2, 14] that the driving agent that implements the upward displacement of the material filling the pipes is water vapor, which forms when kimberlite magma reaches the Earth's crust horizons saturated with water.

From the aforesaid, it follows that the indicated mechanisms presumably resulting in the formation of KPs are constant in the geologic history of the Earth. The tectonic fracture of crustal rock is developed everywhere, and the presence of molten magma saturated with gases in the upper mantle is proved by volcanic activity. Stress corrosion, an adsorption decrease in hardness, and rock dissolution are continuously operating processes.

At first glance, KPs should permanently form in the Earth's crust. However, the age of the pipes found at present is not less than 59 millions years [4]. As follows from geological data, KPs formed in particular time

intervals separated by long periods of "silence." The indicated hypotheses do not explain why KPs do not form in the modern geologic time.

On the scales of continental blocks, the KP channels are the finest "punctures" in the Earth's crust. There is no ground to assume that they were produced in the crust during its formation. Apparently, for some reason, the mechanism of their formation should activate from time to time. For a long time after formation, such channels have been exhibiting increased permeability and are potential paths for the emergence of plutonic rocks. On reaching particular conditions, mantle rocks rush into the channels, fill them, and form the body of the pipes. The mechanism of channel formation can involve wave processes due to impacts of rather large cosmic bodies; this is typical of a change of geologic times.

Zones with intense fracturing, shaped like elongated round cones, form upon focusing of intense seismic surface waves. Such waves are produced by impact of rather large cosmic bodies (asteroids, comets, and their fragments) on the Earth. Propagating along the Earth's surface, these waves are focused in the region that is diametrically opposite to the impact region — the antipode region. In this region, vertically oriented failure channels form in crustal rocks. They are filled with failed rock and are potential routes for kimberlite magma ascent to the Earth's surface.

The reason for the formation of failure channels in rocks is the stress buildup in a convergent surface wave (Rayleigh wave) and formation of ruptures upon wave focusing. It should be noted that similar cumulative phenomena take place, for example, upon focusing of convergent acoustic and shock waves, tsunami wave arrival at the coastal shelf, convergence of a conical envelope in a shaped charge, etc. (see, for example, [1]).

Rock failed by convergent waves exhibits increased permeability to fluids from the upper mantle. This leads to disturbance of equilibrium that existed before wave focusing between lithostatic stresses, on the one hand, and the weight of the rock column and the forces of its cohesion with the ambient medium, on the other hand. In what follows, failed rocks that are not hold by cohesion forces are carried upward by uprising kimberlite fluid.

In the present paper, we consider focusing of surface Rayleigh waves (R-waves), which appear to play a key role in the initiation of KP formation.

Parameters of a Convergent Rayleigh Wave Produced by Impact of a Cosmic Body on the Earth. The parameters of a Rayleigh wave converging to the antipode point can be assessed quantitatively using the analogy between a high-velocity impact and an explosion. These phenomena are similar in the nature of mechanical processes involved in them. Therefore, in a certain approximation, it can be assumed that the impact is similar to an effective explosion with a particular energy and depth. This problem requires additional investigation. In the present paper, we restrict ourselves to rough estimates of the initial parameters of a surface wave.

The fraction of the impact energy E_s converted to seismic energy is proportional to the kinetic energy of the impacting body: $E_\mathrm{s} = k_\mathrm{s}E_\mathrm{k}$ [E_k is the kinetic energy of the impacting body and $k_\mathrm{s} = 10^{-3}$–10^{-5} is the seismic efficiency of the impact, i.e., the fraction of the impact energy converted to the energy of seismic motion). It is common to set $k_\mathrm{s} = 10^{-4}$ [15]. The seismic efficiency of an explosion depends on the type of ground in which it occurs; it is 0.1% for alluvium and 5% for granite [16]. In our case, as the seismic efficiency of an explosion in the indicated range, we use the average value $k_{\mathrm{s,exp}} = 10^{-2}$. Thus, we assume that the seismic efficiency of an impact is approximately 100 times lower than the seismic efficiency of an explosion. This estimate is rather rough; therefore, in what follows, the parameter k_s should be determined more exactly.

Next, we assume that for an impact and an explosion, the energy distribution between volume and surface waves is identical. Apparently, this assumption also leads to a certain underestimation of the intensity of an R-wave because even qualitative analysis shows that an impact of a cosmic body on the Earth is a more effective generator of surface waves than an underground explosion.

Seismic surface waves were discovered by Rayleigh [17]. Information on their properties is also contained in [18, 19] and other papers. Some of them are listed below.

1. In an R-wave, the medium moves in a subsurface layer with thickness on the order of the wavelength λ.

2. Particles of the medium move on elliptic trajectories, so that at the wave front,they begin to shift toward the wave source.

3. With increase in the distance r traveled by the wave, the amplitude of the wave generated by a concentrated source falls off as $r^{-1/2}$.

4. As the depth z increases, the displacement amplitude decreases as follows. The horizontal displacement component decreases under a linear law to the depth $z \approx \lambda/4$, at which its sign changes. After that, it increases and then decreases exponentially. At $0 \lesssim z \lesssim \lambda/4$, the vertical displacement component is almost constant, and at

$z \gtrsim \lambda/4$, it decreases exponentially. Because of a change in the sign of the horizontal displacement component at $z \gtrsim \lambda/4$, the direction of particle rotation becomes opposite.

5. As the depth of the source ($z = z_0$) increases, the wave amplitude decreases exponentially.

6. In the case of an R-wave generated by an explosive source, the displacement of the surface of the medium with time has the form of a single wave pulse (wave packet). The dependences of the oscillation amplitude on the distance to the epicenter and the depths of the observation point and the source and the particle trajectory shapes are qualitatively similar to those for a harmonic wave, whose fundamental period is approximately equal to the duration of a pulsed R-wave.

7. In an R-wave propagating along the surface of a homogeneous, perfectly elastic sphere, motion is approximately symmetric about the cross section of the large circle perpendicular to the axis passing through the source and its antipode. On the segment between the source and the circumference of the large circle, the amplitude of the R-wave falls off as $r^{-1/2}$ (r is the distance from the source reckoned along the surface of the sphere). When the wave passes through the circumference of the large circle and approaches the antipode point, the amplitude increases under the same law $r^{-1/2}$, but r now is the distance along the surface of the sphere from the wave front to the antipode point. In addition, the phase of oscillation of the vertical component about the antipode is shifted by 180° relative to the oscillation phase near the source, which is supported by the data presented Figs. 1 and 2 taken from [18]. Figure 1 gives displacements in an R-wave versus time at two points on the surface of a homogeneous elastic sphere of radius $a = 6400$ km; the points are symmetric about the cross section of the large circle and are separated from the source and its antipode by a distance equal to 1100 km. In this case, the angular distance is $\theta = 10°$. Figure 2 shows the particle trajectories at the indicated points. The source is an explosion generating a longitudinal P-wave. The source is at a depth $z_0 = 1$ km from the surface of the sphere.

In Fig. 1, the dimensionless time $c_S t/a$ is plotted on the abscissa [a is the radius of the sphere (Earth); c_S is the rate of propagation of S-waves in the medium; and t is the time reckoned from the moment of explosion]. The vertical (U_R) and horizontal (U_θ) displacement components are plotted on the ordinate; they are measured on the A^3/a^2 scale (A is a parameter that has the dimension of length). Spherical coordinates (R, θ, φ) are used. The motion is considered axisymmetric.

In [18], the value of the parameter A is not given. Comparing the value of the source function used in [18] with that obtained in [16] for an underground nuclear explosion, we have $A \approx 5 \cdot 10^3$ m. In this case, the scale factor is $A^3/a^2 \approx 3 \cdot 10^{-3}$ m, which corresponds to an explosion energy $E_0 \approx 7.5 \cdot 10^{20}$ J. The data in Figs. 1b and 2b can be used as the initial parameters for a convergent R-wave when studying its further convergence to the antipode.

From Figs. 1 and 2, it follows that the particle trajectories in the R-wave differ little from circular trajectories, i.e., the amplitude of the displacement components are approximately equal: $|U_\theta/U_R| \approx 0.8$. Therefore, in what follows, any of them or, for example, their half-sum $U = (U_R + U_\theta)/2$, is used as the R-wave amplitude. As the wavelength, we use the quantity $\lambda = c_S T$ (T is the doubled time interval Δt between the principal extrema on the curve of displacement versus time).

In the neighborhood of the antipode, we use local cylindrical coordinates (r, z, φ) with origin at the antipode point A. The z axis is directed to the center of the sphere, the plane of values of r lies in the plane tangent to the sphere at the point A. In this case, $r > 0$, $z \geqslant 0$, and $0 \leqslant \varphi \leqslant 2\pi$.

From the geometry of the problem and the nature of R-wave motion along the sphere surface, it follows that near the antipode, the wave is a cylindrical convergent wave and its motion does not depend on the angular coordinate φ. The wave focusing axis is a straight line that passes through the impact point and the antipode point.

The displacement amplitude u and the displacement rate v for the points located on the Earth's surface in the neighborhood of the antipode can be represented as

$$u = u_1(r_1/r)^{1/2}, \qquad v = v_1(r_1/r)^{1/2}, \tag{1}$$

where r is the distance from the antipode point to the wave front and u_1 and v_1 are the displacement and velocity amplitudes at the point $r = r_1$.

As the initial values of u_1 and v_1, we use the Rayleigh wave amplitudes calculated in [18] for a distance from the antipode point $r_1 \approx 1100$ km. The characteristic values of u_1 and the interval Δt between the neighboring extrema on the dependence $u = u(t)$ are determined from Fig. 1b and Fig. 2b: $u_1 \simeq 7.5$ m and $\Delta t \approx 0.02a/c_S \approx 36$ sec. Knowing Δt, we find the oscillation period $T = 2\Delta t \simeq 72$ sec and, setting the velocity of transverse waves $c_S \simeq 3.55$ km/sec, we obtain $\lambda = c_S T \simeq 250$ km. The displacement rate is estimated from the formula $v_1 = 2u_1/\Delta t \simeq 0.04$ m/sec.

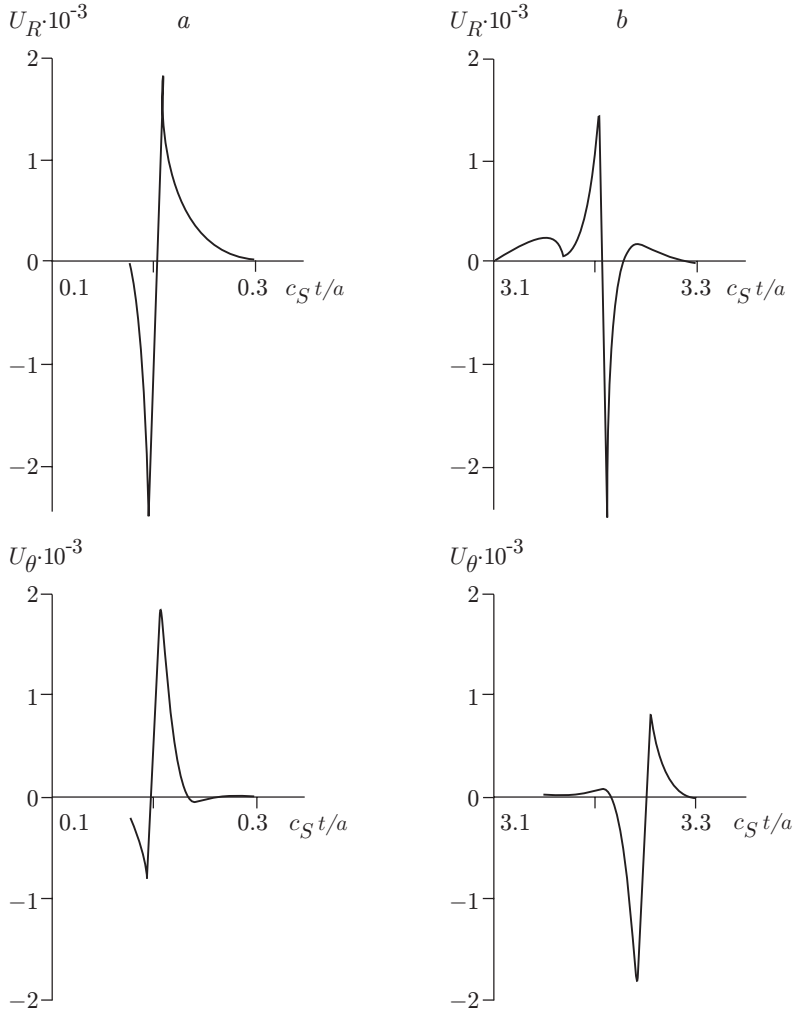

Fig. 1. Displacement of the Earth's surface in a Rayleigh wave versus time near the source (a) and the antipode(b).

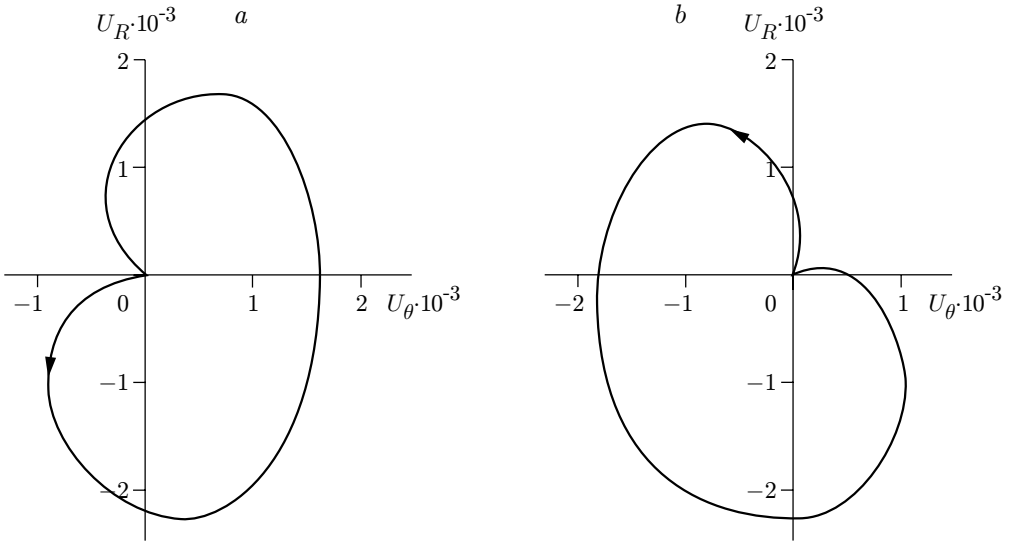

Fig. 2. Particle trajectories in a Rayleigh wave near the source (a) and the antipode (b).

The stress state of the medium is defined by the stress tensor $\hat{\sigma}$:

$$\hat{\sigma} = \sigma_r \boldsymbol{n}_r \boldsymbol{n}_r + \sigma_z \boldsymbol{n}_z \boldsymbol{n}_z + \sigma_\varphi \boldsymbol{n}_\varphi \boldsymbol{n}_\varphi + \sigma_{rz} \boldsymbol{n}_r \boldsymbol{n}_z.$$

Here $\boldsymbol{n}_r$, $\boldsymbol{n}_z$, and $\boldsymbol{n}_\varphi$ are the basis vectors of the cylindrical coordinate system attached to the antipode point.

In a convergent R-wave, the amplitudes of the stress tensor have the same order of magnitude. Therefore, we estimate the stress from the value of the stress component σ_φ leading to radial fractures in the medium upon R-wave focusing:

$$\sigma_\varphi = 2\rho c_S^2 \Big(\frac{u_r}{r} + \frac{\nu}{1-2\nu} \operatorname{div} \boldsymbol{u} \Big).$$

Here $\boldsymbol{u} = u_r \boldsymbol{n}_r + u_z \boldsymbol{n}_z$ is the displacement vector.

In the expression for $\operatorname{div} \boldsymbol{u}$, the values of the derivative $\partial u_z / \partial z$ are small, according to the properties of R-waves considered above; therefore,

$$\operatorname{div} \boldsymbol{u} = \frac{\partial u_r}{\partial r} + \frac{u_r}{r} + \frac{\partial u_z}{\partial z} \approx \frac{\partial u_r}{\partial r} + \frac{u_r}{r} \equiv \frac{\partial u}{\partial r} + \frac{u}{r}.$$

In view of the above remark on the closeness of values of u_r and u_z, we consider only the component u_r, omitting the subscript for brevity. Then, the growth in the stress amplitude in a convergent R-wave is approximately described by the expression

$$\sigma_\varphi \approx 2\rho c_S^2 \Big[\frac{u}{r} + \frac{\nu}{1-2\nu} \Big(\frac{\partial u}{\partial r} + \frac{u}{r} \Big) \Big] \approx \rho c_S^2 \, \frac{2-3\nu}{1-2\nu} \, \frac{u_1}{r_1} \Big(\frac{r_1}{r} \Big)^{3/2} = \sigma_1 \Big(\frac{r_1}{r} \Big)^{3/2}, \tag{2}$$

where $\sigma_1 = \rho c_S^2 [(2-3\nu)/(1-2\nu)] u_1 / r_1$.

In estimating the Rayleigh wave parameters, we use the following averaged characteristics of the Earth's crust: density $\rho = 2.84$ g/cm^3, propagation rate of longitudinal waves $c_{\text{long}} = 6.30$ km/sec, propagation rate of transverse waves $c_S = 3.55$ km/sec, Poisson's constant $\nu = 0.27$, and thickness of the Earth's crust $H = 33$ km. Then, for a reference explosion at a distance $r = r_1 = 1100$ km from the antipode point, the characteristic stress in the convergent surface wave is $\sigma_\varphi \Big|_{r=r_1} = \sigma_1 = 0.65$ MPa.

Using the obtained characteristic values for the explosion, we calculate the R-wave parameters u_1, v_1, and σ_1 at $r_1 = 1.1 \cdot 10^6$ m and $z_0 = 10^3$ m for an impact of a body with a kinetic energy $E_{\text{k}} = 4.2 \cdot 10^{18}$ J. In the calculation, we take into account that according to the above assumption, the seismic efficiency of the impact is approximately 100 times lower than the seismic efficiency of the explosion, i.e., the linear and time scales should be reduced by a factor of $(180 \cdot 100)^{1/3} \approx 26$. Then, for the given scales, we obtain

$$\begin{gathered} \bar{u}_1 = 1.8 \cdot 10^{-7} \text{ m/J}^{1/3}, \qquad \bar{v}_1 = 0.40 \text{ m/sec}, \qquad \sigma_1 = 0.65 \text{ MPa}, \\ \bar{\lambda}_1 = 6.6 \cdot 10^{-3} \text{ m/J}^{1/3}, \qquad \bar{T} = 1.68 \cdot 10^{-6} \text{ sec/J}^{1/3} \\ \text{at} \qquad \bar{r}_1 = 2.5 \cdot 10^{-2} \text{ m/J}^{1/3}, \qquad \bar{z}_0 = 2.3 \cdot 10^{-6} \text{ m/J}^{1/3}, \end{gathered} \tag{3}$$

and for an arbitrary energy E expressed in joules, we have

$$\begin{gathered} u_1 = 1.8 \cdot 10^{-7} E^{1/3} \text{ [m]}, \qquad v_1 = 0.40 \text{ m/sec}, \qquad \sigma_1 = 0.65 \text{ MPa}, \\ \lambda_1 = 6 \cdot 10^{-3} E^{1/3} \text{ [m]}, \qquad T = 1.68 \cdot 10^{-6} E^{1/3} \text{ [sec]} \\ \text{at} \qquad r_1 = 2.5 \cdot 10^{-2} E^{1/3} \text{ [m]}, \qquad z_0 = 2.3 \cdot 10^{-6} E^{1/3} \text{ [m]}. \end{gathered} \tag{4}$$

Estimate of Energy Dissipation. The R-wave amplitude decreases not only because of the geometrical divergence but also because of scattering on heterogeneities and internal friction in the medium. If the properties of the crustal material differ slightly from the properties of a perfectly elastic body, the total attenuation of the wave amplitude can be estimated as follows. In formulas (1) and (2), we introduce an additional factor of the form $\exp[-\alpha(T) l]$, where $\alpha(T)$ is the attenuation factor for oscillations with period T and l is the distance traveled by the wave. The coefficient α is expressed in terms of the dissipation function Q^{-1} (Q is the mechanical quality factor of the oscillating system), the group velocity c_R of the wave packet, and the oscillation period T by the well-known formula

$$\alpha = \pi / (c_R T Q). \tag{5}$$

TABLE 1

T, sec	c_R, km/sec	λ, km	$Q \cdot 10^{-2}$	$\alpha \cdot 10^4$, km^{-1}	$\exp(2 \cdot 10^4 \alpha)$
12	3.10	37	5.10	1.67	28.0
23	3.10	71	3.10	1.40	16.4
43	3.60	155	2.50	0.81	5.1
72	3.80	270	1.25	0.92	6.2
108	3.75	400	1.00	0.78	4.8
215	3.70	800	0.94	0.42	2.3

For crustal rocks, Q and c_R are also functions of T. The dependences $Q(T)$ and $c_R(T)$ for the fundamental harmonic of Rayleigh waves in the continental crust are calculated in [19]. Values of the coefficient α calculated from formula (5) using the data of [19] are presented in Table 1. The data given in the last column of Table 1 show how many times the R-wave amplitude decreases when the wave travels the distance from the impact point to the antipode ($l = 2 \cdot 10^4$ km). For example, an R-wave with a period $T = 43$ sec and a wavelength $\lambda = 155$ km is attenuated by a factor of 5 and a wave with $\lambda = 800$ km, by a factor of 2.3. Thus, the law of geometrical similarity for impacts of different scales is violated because of dissipation losses. A correction into the wave parameters needs to be introduced for each impact, depending on the impact strength. This can be done using the data of Table 1.

In view of dissipation losses, the formulas for the amplitude parameters of a convergent R-wave become

$$u = u_1(r_1/r)^{1/2}\exp[-\alpha(\pi a - r)], \qquad v = v_1(r_1/r)^{1/2}\exp[-\alpha(\pi a - r)],$$
$$\sigma = \sigma_1(r_1/r)^{3/2}\exp[-\alpha(\pi a - r)], \tag{6}$$

where the attenuation factor $\alpha = \alpha(T)$ is defined by expression (5) and a is the Earth's radius. In the neighborhood of the antipode, $r \ll \pi a$; therefore, neglecting the second term in the exponent, we obtain

$$u = u_1(r_1/r)^{1/2}\exp[-\alpha(T)\pi a], \qquad v = v_1(r_1/r)^{1/2}\exp[-\alpha(T)\pi a],$$
$$\sigma = \sigma_1(r_1/r)^{3/2}\exp[-\alpha(T)\pi a], \tag{7}$$

where the values of the parameters u_1, v_1, σ_1, T, and r_1 are given by expressions (4).

Rock Failure in the Neighborhood of the Antipode. A Rayleigh wave moves over the Earth's surface to the antipode as a circular bar, whose diameter $2r$ decreases and vanishes upon focusing. The height of the bar (surface displacement amplitude) increases as $r^{-1/2}$, the stress and strains increase as $r^{-3/2}$, and the elastic energy density increase as r^{-3} for $r \to 0$. In this case, motion in the subsurface layer of the Earth propagates to a depth approximately equal to the length of the R-wave. Thus, the seismic perturbation converges as a cylindrical wave to the focusing axis. At the wave front, the ground begins to move from the focusing axis, extending in the radial, azimuth, and vertical directions. The process of wave convergence leads to stress buildup, and at a certain distance from the focusing axis $r = r_*$, the stresses exceed the ultimate strength of the ground, resulting in fracture and failure of the ground.

The system of cracks that arises at $r = r_*$ moves together with the wave to the focusing axis, and the boundary $r = r_*$ moves in the opposite direction. The fractured rock moves away from the axis. As a result, a cylindrical cavity converging with increase in the depth exists along the focusing axis for a time; the wall of the cavity consists of failed rocks. The slope of the wall is greater than the natural slope of the failed rocks. Therefore, fragments of disintegrated rocks fall down under gravity.

We estimate the dimensions of the failure zone r_*, the lifetime of the cavity t_*, the radius of the cavity r_h, and the depth of fall of rock fragments z_*. Let $\sigma = \sigma_*$ be the failure strength of the rock. At a distance from the antipode $r = r_*$, radial cracks begin to form provided that

$$\sigma = \sigma_1(r_1/r)^{3/2}\exp[-\alpha(T)\pi a] = \sigma_* + \sigma_g \tag{8}$$

($\sigma_g = \rho g z$ is the lithostatic pressure at a depth z and g is the acceleration of gravity).

From (8), we obtain

$$r_* = r_1\Big(\frac{\sigma_1\exp[-\pi a\alpha(T)]}{\sigma_* + \rho g z}\Big)^{2/3}. \tag{9}$$

The displacement u_* and velocity v_* of the boundary $r = r_*$ are given by the relations

$$u_* = u_1\Big(\frac{r_1}{r_*}\Big)^{1/2}\exp\left[-\alpha(T)\pi a\right] = u_1\Big(\frac{\sigma_* + \rho g z}{\sigma_1}\Big)^{1/3}\exp\Big[-\frac{2}{3}\,\pi a\alpha(T)\Big]; \tag{10}$$

$$v_* = u_1\Big(\frac{\sigma_* + \rho g z}{\sigma_1}\Big)^{1/3}\exp\Big[-\frac{2}{3}\,\pi a\alpha(T)\Big]. \tag{11}$$

The maximum radius of the cavity at the free-surface level can be estimated using the law of conservation of mass. In a layer of unit thickness, the rock displaced from the boundary $r = r_*$ releases a volume equal to $2\pi r_* u_*$, which, in turn, is equal to the volume of the cavity near the focusing axis πr_h^2. From this condition, using relations (9) and (10), we obtain

$$r_h = 2(r_* u_*)^{1/2} = 2(r_1 u_1)^{1/2}(\sigma_1/\sigma_*)^{1/6}\exp\left[-(2/3)\pi a\alpha(T)\right]. \tag{12}$$

The lifetime of the cavity is approximately equal to the duration of the tension phase in the R-wave:

$$t_* = 2u_*/v_* = 2u_1/v_1 = 10^{-6}E^{1/3}\ \text{[sec]}. \tag{13}$$

As the cavity is expanded, the fractured rock disintegrates into fragments, which fall down until the converging cavity walls wedge them at a certain depth z_*. In time t_*, the fragments fall down to a depth

$$z_* = gt_*^2/2 = 2g(u_1/v_1)^2 = 0.5\cdot 10^{-12} g E^{2/3}. \tag{14}$$

Example 1. Let a cosmic body with a density $\rho = 2750$ kg/m^3 and a radius $r_0 = 1$ km impacts the Earth at a velocity $V = 20$ km/sec. The kinetic energy of the body is

$$E = mV^2/2 = (4/3)\pi\rho r_0^3/2 = 2.3\cdot 10^{21}\ \text{J}.$$

According to (4), the oscillation period in the impact-generated R-wave is $T = 23$ sec. This corresponds to a wavelength $\lambda = 71$ km. In Table 1, we find the attenuation factor $\alpha = \alpha(T) = \alpha(23) = 1.4\cdot 10^{-4}$ km^{-1} and the exponential factor $\exp\left[\pi a\alpha(T)\right] = \exp\left[2\cdot 10^4\alpha(T)\right] = 16.4$.

The characteristic tensile strength of rock is $\sigma_* \approx 30$ MPa. Then, with allowance for (4) and relations (9)–(14), the radius of the failure zone near the surface ($z \approx 0$) is $r_* \simeq 4180$ m, the displacement of the failure boundary is $u_* \simeq 1.37$ m, the velocity of the failure boundary is $v_* \simeq 0.224$ m/sec, the cavity radius is $r_h \simeq 106$ m, the lifetime of the cavity is $t_* \simeq 12.3$ sec, and the depth of fall of rock fragments is $z_* \simeq 740$ m.

The process considered (formation of a conical region of fractured rock and a cavity) occurs at a depth less than quarter of the Rayleigh wavelength. Below this level, the action of the wave begins with a compression phase; i.e., the material moves to the focusing axis and is compressed. The model of an elastic body is not suitable for studying this region of motion. It is necessary to take into account the plastic properties of crustal rocks. We describe the subsequent processes qualitatively.

After termination of the tension phase above the level $z \approx \lambda/4$, the rock begins to move to the focusing axis and is compressed. Rock failure continues, and transition to a plastic state is possible. The law wave convergence changes but the energy concentration near the focusing axis continues to increase, though to a lesser extent than in an elastic wave [1]. In this process, a ground stream in the form of an upward directed jet can form, resulting in ejection of the ground from the region adjacent to the focusing axis. At the same time, the material below the level $z \approx \lambda/4$ begins to stretch. This can lead to material failure and formation of a cavity in the form of a cone diverging with increase in the depth. The lower cavity, like the upper one, exists for a time $t_* \simeq 10^{-6}E^{1/3}$. Closure of the lower cavity can result in uprise of crustal rocks.

If the impact energy is high enough, and, accordingly, the wavelength λ is great enough, the failed crustal rock pipe can penetrate into the mantle. The failed rock channel that formed is the primary channel through which the mantle material in the form of kimberlite magma can rise to the Earth's surface and form a kimberlite pipe.

Therefore, the condition of KP formation is the following: the length of the R-wave converging to the antipode should be greater than the thickness of the Earth's crust. Using the expression from (4) for the wavelength, we find that the kinetic energy of the impacting body should be

$$E \gtrsim 4.6\cdot 10^6 H^3,\ \text{J}$$

(H in meters).

Effect of the Earth's Inhomogeneity. The approximate estimates obtained for the parameters of a convergent R-wave and its effect on crustal rock in the neighborhood of the antipode are valid for a homogeneous

elastic sphere. The Earth is inhomogeneous: the density and velocity of seismic waves basically increase with increase in the depth. Therefore, the seismic rays of P- and S-waves issuing from the place of impact are curved. Some of them are reflected from the boundary of the mantle and again enter the crustal layer. The other move toward the free surface and are reflected from it. Each reflection gives rise to new R- and R-waves and surface R-waves. The number of reflected waves increases in geometrical progression. They interfere, so that a considerable portion of the motion energy is concentrated in a subsurface waveguide near the free surface. As a result, a system of surface interferential waves (Rayleigh, Lové, etc., waves) forms in the crustal layer.

As in the case of a homogeneous sphere, the amplitudes of surface waves propagating from the source to the cross section of the large circle decrease because of geometrical divergence. After passage through the cross section of the large circle, the wave amplitudes increase as a result of convergence.

In this process, the nature of oscillations in Rayleigh waves changes. Instead of a single pulse, a train of quasiharmonic oscillations propagates, followed by irregular, higher-frequency oscillations. Surface waves increasing in amplitude are incident one after another on the antipode region. Their aggregate action on crustal rocks is apparently stronger than that in the case of a homogeneous sphere.

The Earth's nonsphericity and the azimuthal-latitude inhomogeneity of the lines of propagation of seismic surface waves can lead to deformation of the wave fronts and angular heterogeneity of the wave amplitudes. The front of a convergent wave can assume a rather complex shape, and focusing of such a front can occur along several axial lines. Probably, focusing of subsequent R-waves in the train occurs in places that do not coincide with the places of focusing of previous waves. As a result, a set of channels of failed rocks can arise in the neighborhood of the antipode. Intrusion of kimberlite magma into them can led to the formation of a KP field.

It is not only surface waves that facilitate and stimulate kimberlite magma intrusion along the failure channels. In the deeper regions of the mantle adjacent to the axis passing through the impact region and its antipode, a large number of other seismic waves is focused. Their collision and interaction with the rocks of the Earth's crust and mantle lead to effective dissipation of seismic energy and its conversion to heat. Even a slight increase in rock temperature increases the mobility of the rocks and accelerates recrystallization processes involving heat release [3]. Apparently, these deep-seated processes are responsible for the mobility of the mantle material in the foundation of kimberlite provinces. Subsequent motion of this material upward and along the normal to the axis of the antipode results in sequential filling of the failure channels produced earlier by weaker impacts. The proposed scenario is hypothetical. Its justification requires additional studies.

Conclusions. The KP formation mechanism considered in the present paper explains many features of the morphology of the pipes and enclosing rocks, for example, the shapes of the pipes, the presence of detrital material of the upper layers of enclosing rocks at a depth, the brecciation of kimberlites, the metamorphism of xenoliths, the occurrence of pipe fields, etc. The proposed scenario of KP formation allows for extension of failure channels to the Earth's mantle and entrapment and advance of the mantle material (kimberlite) along the channel produced by an R-wave to the day surface. The cumulation of seismic surface waves is a common mechanism that initiates formation not only of kimberlite pipes but also of some other forms of diatremes.

One might expect that the number of KP fields on the Earth is equal to the number of large impact craters and ring structures and the number of diatreme fields is determined by the number of weaker impacts. A considerable portion of diatreme fields could have been masked by active geologic processes.

Cryptoexplosion structures and circular structures should be located, with allowance for global tectonic motions, in the antipode regions of the well-known diamond-bearing provinces. However, detecting them is a difficult problem because it requires allowance for the motion of the Earth's crust. On modern maps, the South African diamond province corresponds to the region of the Pacific Ocean to the south of the Hawaiian islands, the Yakut province corresponds to the region of the Weddell sea near the coast of Antarctica, and the Brazilian province corresponds to the region of the Pacific Ocean between the Philippine and Mariana islands.

The aforesaid suggests that KPs and generally diatreme fields are evidence for the bombardment of the Earth by cosmic bodies. The biggest impacts were responsible, apart from formation of particular diatreme fields, for the formation of mantle underflows, which, in turn, led to filling of the previously produced channels with the mantle material. It is of interest to develop a program of integrated studies of crustal movement, the formation of impact craters and cryptoexplosion structures, and the genesis of diatreme fields. Results of such studies could make a significant contribution to the reconstruction of the geological past of the Earth. Valuable results can be obtained from studies of such phenomena on other terrestrial planets. On some of them, failures in the impact antipode regions might be more pronounced by virtue of the lower intensity of geological processes.

REFERENCES

1. E. I. Zababakhin and I. E. Zababakhin, *Phenomena of Unlimited Cumulation* [in Russian], Nauka, Moscow (1988).
2. V. A. Milashev, *Kimberlites and Plutonic Geology* [in Russian], Nedra, Leningrad (1990).
3. J. Ferhugen, F. Terner, L. Weiss, et al., *The Earth. An Introduction to General Geology*, Holt–Rinehart–Winston, New York (1970).
4. J. B. Dawson, *Kimberlits and Their Xenolithes,* Springer-Verlag (1980).
5. I. D. Ryabchikov and I. T. Rass, "Molten carbonates in the Earth's interior," *Priroda*, No. 8, 67–74 (1998).
6. F. C. Frank, "Defects in diamonds," in: *Proc. of the Int. Industr. Diamond Conf.* (Oxford, 1966), Industr. Diamond Inform. Bureau, London (1967), pp. 119–135.
7. S. V. Belov and A. A. Frolov, "Forerunners of mantle magmas," *Nature*, No. 11, 44–56 (1998).
8. P. A. Wagner, *Die Diamantfuhrenden Gesteine Sudafricas, Ihre Abban und Ihre Aufbereitung*, S. n., Berlin (1909).
9. V. I. Mikheenko, "The mechanism of formation of kimberlite pipes," *Dokl. Akad. Nauk SSSR*, **205**, No. 2, 428–430 (1972).
10. L. A. Novikov and R. M. Slobodskii, "The mechanism of diatreme formation," *Sov. Geolog.*, No. 8, 3–14 (1978).
11. B. M. Vladimirov, S. N. Kostrovitskii, L. V. Solov'eva, et al., *Classification of Kimberlites and the Internal Structure of Kimberlite Pipes* [in Russian], Nauka, Moscow (1981).
12. A. Locke, "The formation of certain ore bodies by mineralization stopping," *Econ. Geol.*, **21**, 431–463 (1926).
13. F. J. Sawkins, "Chemical brecciation an inrecognized mechanism for breccia formation," *Econom. Geol.*, **64**, 613–617 (1969).
14. V. Lorenz, *Formation of Preatomagmatic Maar-Diatreme Volcanoes and Its Relevance to Kimberlite Diatremes*, Vol. 9, Pergamon Press, New York (1973), pp. 17–27.
15. H. Melosh, *Impact Cratering. A Geological Process*, Oxford University Press–Clarendon Press, Oxford–New York (1989).
16. N. A. Haskell, "Analytic approximation for the elastic radiation from a contained underground explosion," *J. Geophys. Res.*, **72**, 2583–2588 (1967).
17. Lord Rayleigh (J. W. Stratt), "On waves propagation along the plane surface of the elastic solid," *Proc. London Math. Soc.*, **17**, 4–11 (1885).
18. Z. Alterman and F. Abramovici, "Effect of the depth of a point source on the motion of the surface of an elastic solid sphere," *Geophys. J. Roy. Astron. Soc.*, **11**, 189–224 (1966).
19. A. L. Levshin, "*Surface and Channel Seismic Waves*" [in Russian], Nauka, Moscow (1973).